

Supporting information

Size-controlled synthesis of hierarchical nanoporous iron based fluoride and its high performances in rechargeable lithium ion batteries

Yan Lu, Zhao-yin Wen^a, Jun Jin, Xiang-wei Wu and Kun Rui

CAS Key Laboratory of Materials for Energy Conversion, Shanghai Institute of Ceramics, Chinese Academy of Sciences, Shanghai, China 200050.

1. Experimental details

Materials Preparation

Reagents: 1-butyl-3-methylimidazolium -tetrafluoroborate (BmimBF₄, 99%) was purchased from Shanghai Cheng Jie Chemical Co. Ltd.. Iron (III) chloride hexahydrate (FeCl₃·6H₂O, AR), anhydrous ferric chloride (FeCl₃, AR) and ethanol (C₂H₅OH, AR) were purchased from Sinopharm Chemical Reagent Co. Ltd.. Oleylamine (C₁₈H₃₇N, 70%) used in the synthesis process was obtained from Sigma-Aldrich Co. LLC..

Synthesis process: Size controlled hierarchical nanoporous structured iron based fluorides were synthesized through a facile, one step solvothermal approach using 1-butyl-3-methylimidazolium tetrafluoroborate (BmimBF₄) ionic liquid as fluorine source, iron (III) chloride hexahydrate (FeCl₃·6H₂O) as iron source and oleylamine as the size tuning agent. Specifically, take sample F-0.5 for example, 1g FeCl₃·6H₂O and 1 mL fluorine source BmimBF₄ were firstly dissolved in 30mL ethyl alcohol solvent under stirring at room temperature to form a clear solution A. Then, 0.5 mL oleylamine was added dropwise to solution A under stirring for another 30 min. The mixtures were transferred to a Teflon autoclave, sealed and heated to 120 °C and maintained at this temperature for 10 h. Finally, yellowish white precipitates were washed six times with acetone and centrifuged for 10 min at 10000 rpm to remove residual ionic liquid and other organic impurities, followed by subsequent drying under vacuum at 60 °C for 24 h.

A similar synthesis process was conducted with anhydrous ferric chloride as iron source. In order to verify the influence of hydration water on the products, OAm is absent in the process. Specifically, 1g FeCl₃ and 1 mL fluorine source BmimBF₄ were dissolved in 30mL ethyl alcohol solvent under stirring at room temperature. Then the mixture was transferred to a Teflon autoclave, sealed and heated to 120 °C and maintained at this temperature for 10 h. Finally, the precipitates were obtained by washing and centrifugation with acetone and dried under vacuum as described previously.

Material characterization

Structure and crystallinity of iron-based fluorides were checked by X-ray diffraction (XRD, Rigaku Ultima IV, 40 kV/30 mA, Cu-K α radiation). The morphologies were characterized by scanning electron microscopy (SEM, Magellan-400, FEI) and transmission electron microscopy (TEM, Hitachi, H-800, Japan). High resolution transmission electron microscopy (HRTEM, JEM-2100F) was further used to check the microstructure of the products. X-ray photoelectron spectrometer (Thermo ESCALAB 250) was used to determine chemical bonding energy in the products.

Electrochemical measurements

Working electrodes were prepared by coating the slurry of the as-obtained active materials (60 wt%), acetylene black (20 wt%), and polyvinylidene fluoride (PVDF) (20 wt%) dissolved in n-methyl pyrrolidinone (NMP) onto a alumina foil substrate and dried in a vacuum oven at 80 °C for 2 days. Testing cells were assembled in an argon filled glove box with oxygen and water contents less than 1 ppm. They are fabricated using high-purity lithium foil (China Energy Lithium Co., Ltd) as counter electrode and reference electrode, Celgard 2400 as the separator, and a solution of 1 M LiPF₆ in ethylene carbonate (EC)/dimethyl carbonate (DMC) (1:1, in wt%) as electrolyte in coin type cells. Galvanostatic charge and discharge processes were conducted on a LANDCT2001A battery test system under a voltage range of 1.6 V-4.5 V (versus Li/Li⁺) at different current densities. The current density used is calculated according to the theoretical capacity of 237 mAh g⁻¹ with one electron transfer in the iron based fluorides. That is, 0.1 C represents 23.7 mA g⁻¹, 0.3 C represents 71.1 mA g⁻¹, 1 C represents 237 mA g⁻¹ and so on. All of the electrochemical tests were performed at room temperature and the current density and specific capacity were calculated based on the prepared active materials.

2. Supporting figures

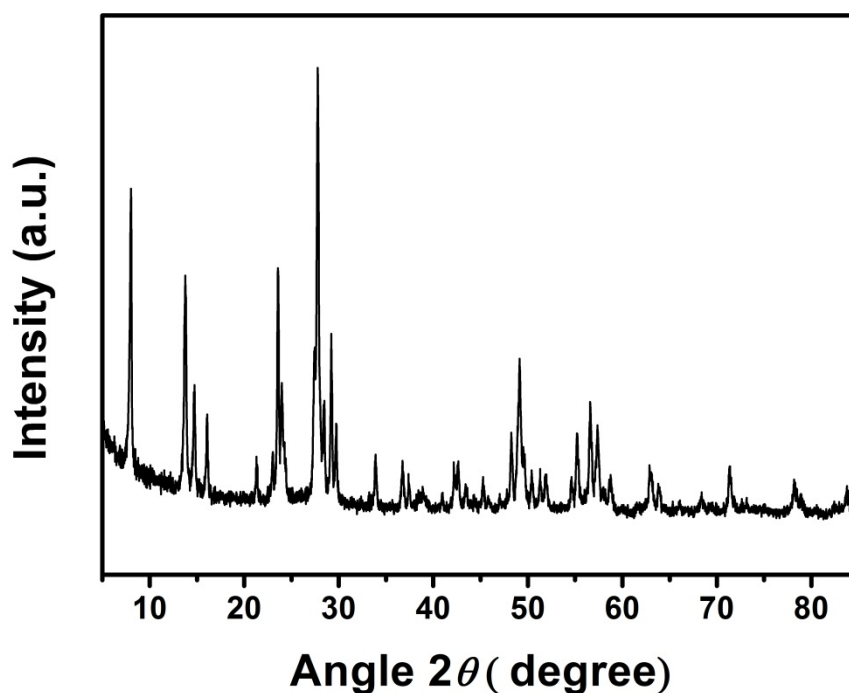


Figure S1. XRD patterns of the products using anhydrous ferric chloride as iron source

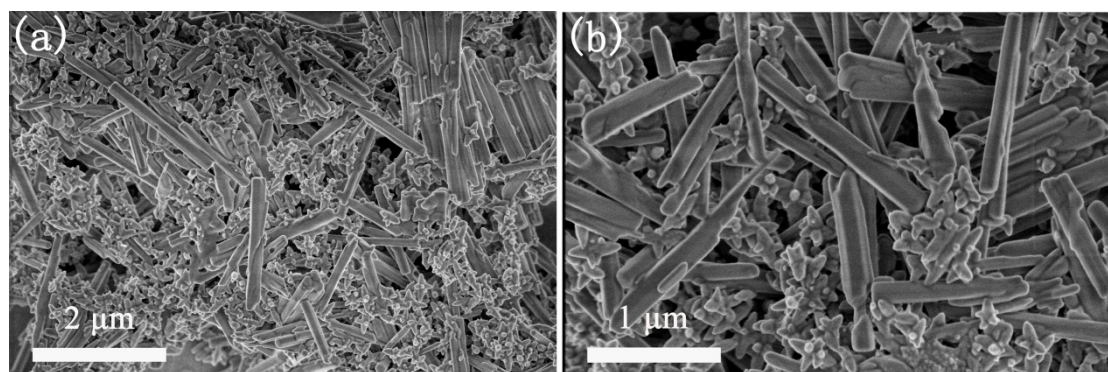


Figure S2. SEM images of the products using anhydrous ferric chloride as iron source

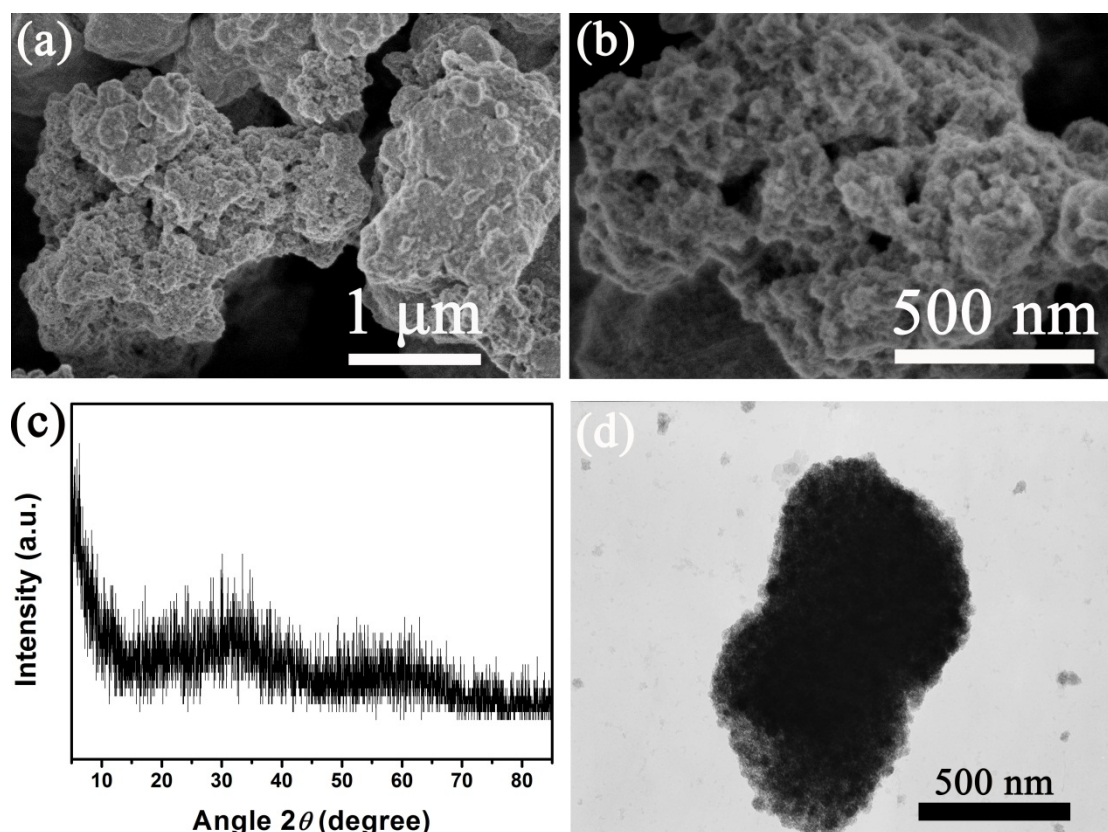


Figure S3. (a,b) SEM, (c) XRD patterns and (d) TEM images of the products with 1 mL OAm

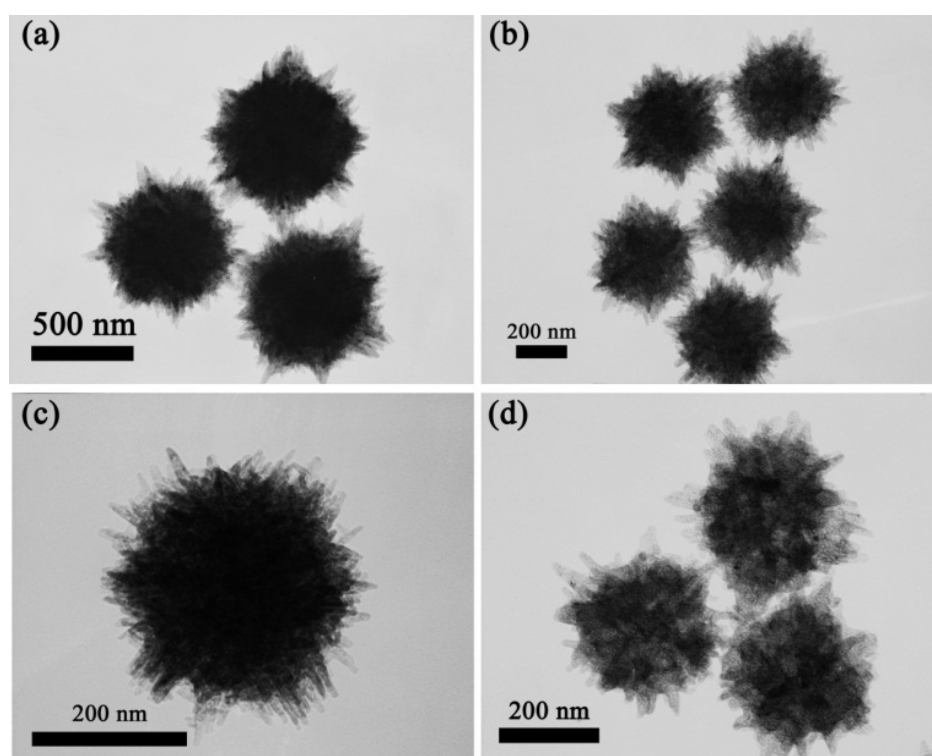


Figure S4. TEM images of the prepared SHIFs with controllable size: F-0 (a); F-0.1 (b); F-0.2 (c); F-0.5 (d).

The details of the morphology changes of the prepared materials are further confirmed by TEM images as Fig. S4 indicated. With the increasing of amount of OAm from 0 mL to 0.5 mL, the structure of SHIFs becomes loose. It is considered that sample F-0.5 with the smallest size and loose structure is more attractive when used as cathode for rechargeable lithium battery due to the following reasons: on one hand, the reduced size of nanorods can short the path lengths for electronic transport and Li^+ transport, beneficial for the improvement of electrochemical activity of insulating electrode materials; on the other hand, voids derived from the assembly of nanorods can provide channels for the impregnation of the electrolyte, which can enlarge the electrode/electrolyte contact area significantly and is beneficial for high charge/discharge rates; besides, the loose structure can efficiently accommodate the volume change of the cathode materials during Li^+ insertion/extraction cycles and thus prevent the pulverization of electrode.

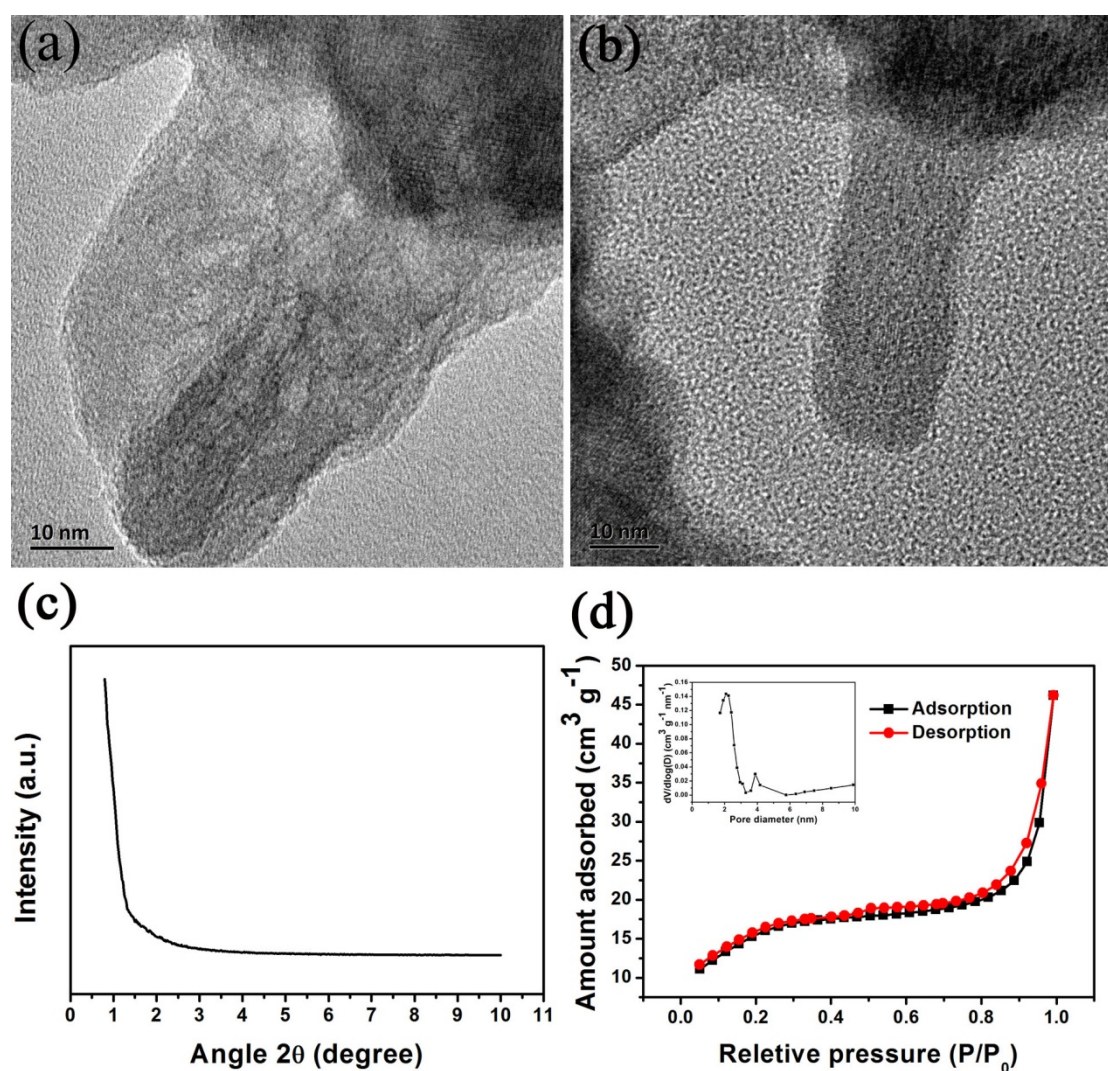


Figure S5. (a,b) HRTEM images, (c) SXPS patterns, nitrogen adsorption-desorption isotherm plot (d) and pore size distribution curve (inset of d) of sample F-0.5.

Small-angle x-ray scattering (SXPS), high-resolution transmission electron microscopy (HRTEM) and nitrogen adsorption-desorption measurement are further used to examine the porous structure of sample F-0.5 as depicted in Fig. S5, from which we can see that the pores in the sample are disordered with no diffraction peaks in SXPS. HRTEM image showed that there is no pores inside iron based fluorides nanorods. Therefore, it is considered that the pores in the sample are derived from the stacking of nanorods. Although the pore size distribution curve

demonstrated that the pore diameters are concentrated in a range of mesoporous scale (2-50 nm), to be accurate, it is called nanoporous structure in this report.

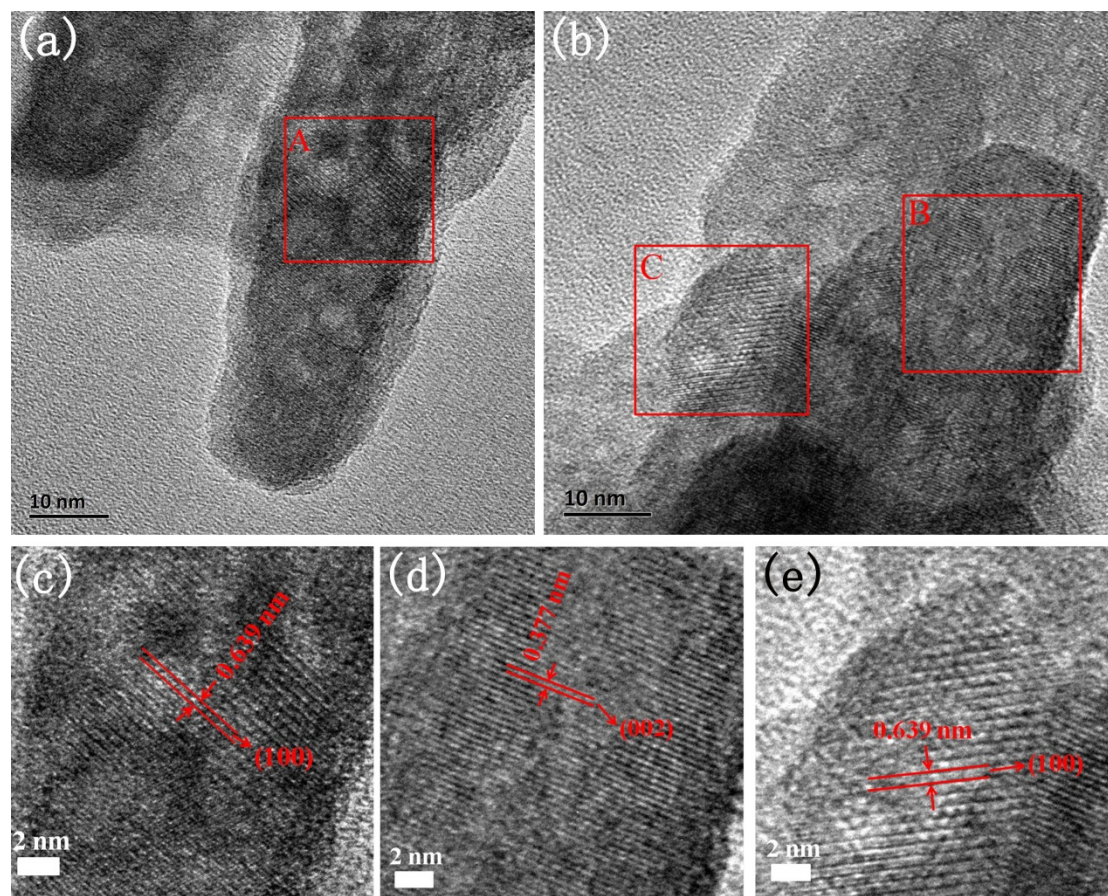


Figure S6. (a, b) HRTEM of the sample F-0.5; HRTEM of the sample F-0.5 in area A (c), area B (d) and area C (e).

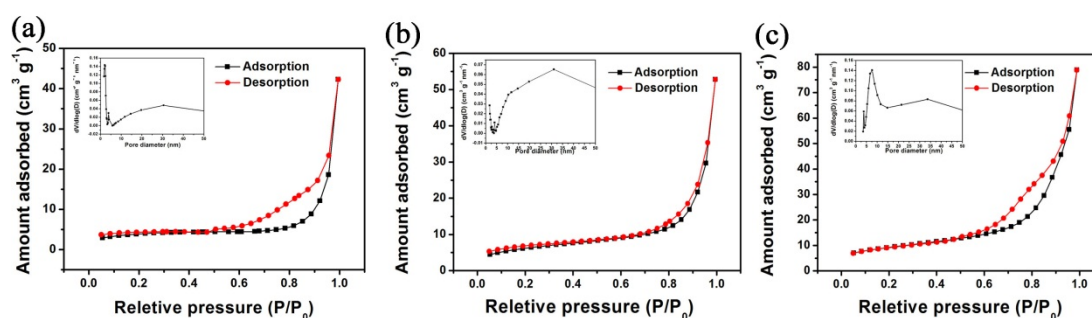


Figure S7. Nitrogen adsorption-desorption isotherm plots and the pore size distribution curves (inset) of sample (a) F-0, (b) F-0.1 and (c) F-0.2

Fig. S7 showed nitrogen adsorption-desorption results of the other three samples (F-0, F-0.1 and F-0.2). All of them exhibited similar nitrogen isotherm curves to that of F-0.5, but there are great differences among their BET surfaces with $13 \text{ m}^2 \text{ g}^{-1}$ for F-0, $22 \text{ m}^2 \text{ g}^{-1}$ for F-0.1, $33 \text{ m}^2 \text{ g}^{-1}$ for F-0.3 and $57 \text{ m}^2 \text{ g}^{-1}$ for F-0.5. The increase of BET surface area with the increasing of the amount of OAm further demonstrated the important role of size tuning agents for SHIFs.

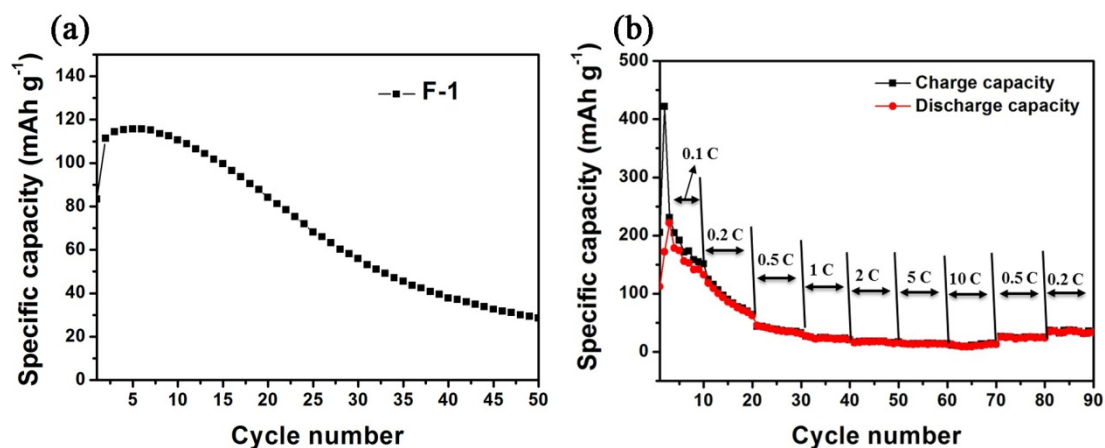


Figure S8. (a) Discharge capacity of the electrodes as a function of cycle number and (b) rate performances of sample F-1.0

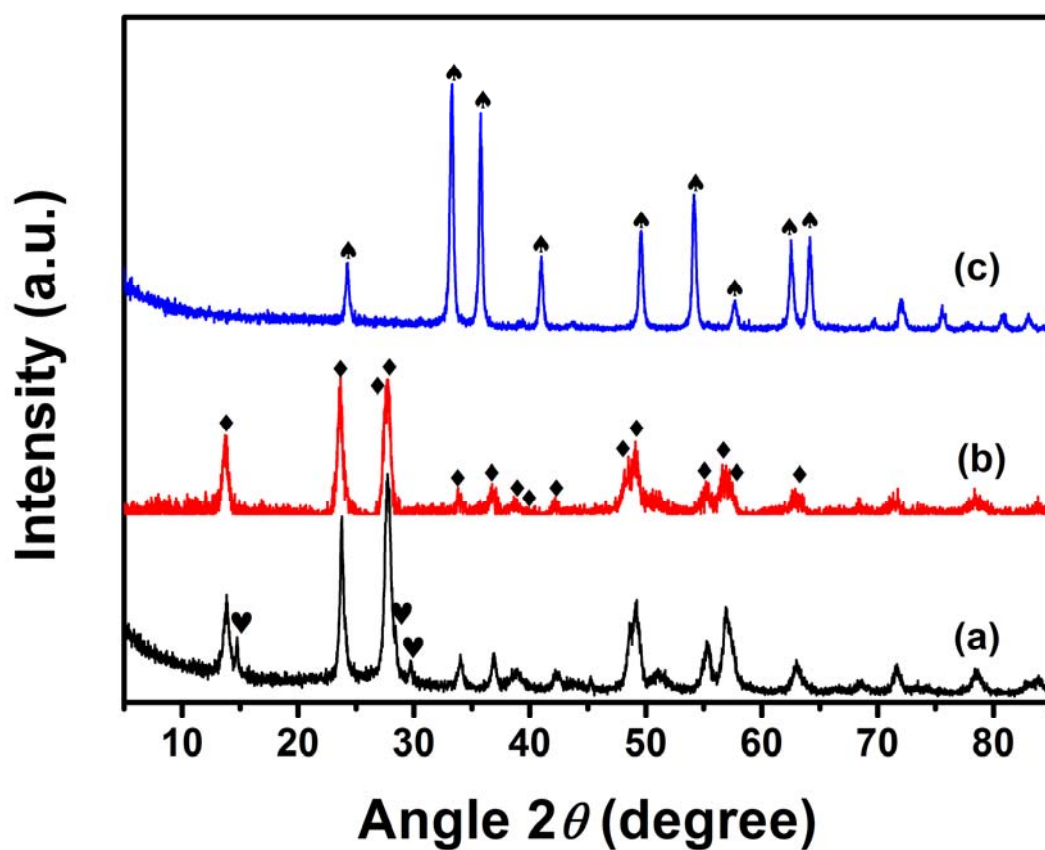


Figure S9. XRD patterns of sample F-0.5 (a), after 300 °C heat treatment (b) and after 450 °C heat treatment (c): heart-shaped: $\text{Fe}_{1.9}\text{F}_{4.75} \cdot 0.95\text{H}_2\text{O}$; diamond: $\text{FeF}_3 \cdot \text{H}_2\text{O}$; spade: $\text{H-Fe}_2\text{O}_3$